

RESEARCH

Open Access



# CAR-NK cells with dual targeting of PD-L1 and MICA/B in lung cancer tumor models

Lingtong Zhi<sup>1\*</sup>, Zikang Zhang<sup>1</sup>, Qing Gao<sup>1</sup>, Chongye Shang<sup>1</sup>, Wenhui He<sup>1</sup>, Yuqing Wang<sup>1</sup>, Changjiang Guo<sup>1</sup>, Zhiyuan Niu<sup>1</sup> and Wuling Zhu<sup>1\*</sup>

## Abstract

**Background** Chimeric antigen receptor (CAR) engineered natural killer (NK) cells have shown their efficacy and superiority against cancer and possess the potential to become off-the-shelf immunotherapy products. Nonetheless, some challenges associated with CAR-NK cells still exist including inhibitory receptor engagement, antigen escape, and inadequate activation.

**Methods** Given this, based on the concept of synthetic biology, we rationally designed a novel dual-targeted CAR (dtCAR), primarily comprising PD-L1 nanoantibody (PD-L1<sup>Nb</sup>) and NKG2D as the ectodomain, transmembrane and cytoplasmic domains (CP) of CD28, and the CP of 4-1BB and CD3ζ. NK92 cells were engineered to express this third-generation of dtCAR. We then elucidated the role of dtCAR-modified NK92 cells against cancer cells in vitro and in vivo.

**Results** In vitro, the dtCAR-NK92 cells could still retain the characteristics of parental NK cells and exhibit improved NK cell cytotoxicity and produce more cytokines than NK92 cells when they were co-cultured with human lung cancer H1299 cells. Notably, the dtCAR-NK92 cell therapy might elicit clearance of H1299 cells by pyroptosis. Additionally, dtCAR-NK92 cells could considerably inhibit tumor growth in the human lung cancer H1299 cell tumor model.

**Conclusions** We confirmed that expression of dtCAR enhanced NK92-cell activation and killing in vitro and in vivo, which provides a novel immunotherapeutic strategy for using NK-tailored CAR-engineered NK92 cells to treat human lung cancer.

**Keywords** NK cells, PD-L1 nanoantibody, NKG2D, Pyroptosis, NK-tailored CAR, Human lung cancer

\*Correspondence:

Lingtong Zhi  
lingtong\_zhi@xxmu.edu.cn  
Wuling Zhu  
wuling\_zhu@163.com

<sup>1</sup>Henan Province Engineering Research Center of Innovation for Synthetic Biology, School of Life Sciences and Technology, Xinxiang Medical University, Xinxiang, Henan, China



© The Author(s) 2025, corrected publication 2025. **Open Access** This article is licensed under a Creative Commons Attribution-NonCommercial-NoDerivatives 4.0 International License, which permits any non-commercial use, sharing, distribution and reproduction in any medium or format, as long as you give appropriate credit to the original author(s) and the source, provide a link to the Creative Commons licence, and indicate if you modified the licensed material. You do not have permission under this licence to share adapted material derived from this article or parts of it. The images or other third party material in this article are included in the article's Creative Commons licence, unless indicated otherwise in a credit line to the material. If material is not included in the article's Creative Commons licence and your intended use is not permitted by statutory regulation or exceeds the permitted use, you will need to obtain permission directly from the copyright holder. To view a copy of this licence, visit <http://creativecommons.org/licenses/by-nc-nd/4.0/>.

## Introduction

Malignant tumors present serious threats to the lives of patients and remain by far the leading cause of death worldwide [1]. The limitations of traditional treatment methods have necessitated an intensified search for new treatment strategies, representing a hotspot in current cancer research. The optimal strategy for tumor therapy aims to overcome immunosuppression within the tumor microenvironment (TME) while simultaneously achieving precise targeting and eradication of cancer cells, thereby ensuring both safety and sustained antitumor effects [2]. Immune cell-driven tumor immunotherapy has introduced fresh perspectives on cancer treatment, with cell-based immunotherapies rapidly emerging as a leading modality in the effective management of malignancies.

Among them, the representative chimeric antigen receptor (CAR)-engineered T (CAR-T) cell therapy involves engineering a patient's T cells and infusing them back into the patient to mediate anti-tumor activities. Notable advancements in CAR-T cell therapy have revolutionized the treatment of hematological malignancies; however, its application in solid tumors faces notable constraints. Moreover, the unique biological and immunological properties of T cells give rise to challenges, including the potentially life-threatening cytokine release syndrome (CRS) [3]. During the clinical administration of CAR-T therapy, nearly all patients exhibit some level of toxicity, which can progress to severe complications, such as heart failure, multi-organ dysfunction, and, in extreme cases, patient mortality. This toxicity profile is a major obstacle hindering the broader application of CAR-T cell therapy [4]. As a more recent alternative, CAR-NK cell therapy represents a novel area within immunotherapy. Compared with CAR-T cell therapy, CAR-NK cells offer several advantages, including the absence of the need for prior sensitization, no restriction by the major histocompatibility complex (MHC), a lower likelihood of causing cytokine storms and graft-versus-host disease (GvHD), and a broader range of sources beyond just autologous NK cells. By applying the design concepts of CAR-T cells to CAR-NK cells, CAR-NK cells could become a dominant treatment modality for next-generation malignant tumors [5].

The programmed death receptor 1 (PD-1)/PD-L1 axis is a prominent target in the realm of malignant tumor therapies, particularly within the advancing field of CAR-T and NK cell therapies. PD-L1, which is ubiquitously expressed on the surface of most tumor cells, facilitates its interaction with PD-1 receptors found on immune cells. This engagement suppresses immune cell activation, thereby reducing the capacity of immune cells to effectively attack cancer cells [6]. The goal of targeting PD-L1 expressed on the surface of cancer cells is to

inhibit its binding to PD-1, effectively obstructing the pathway that suppresses immune cell activation [7].

Nanobodies are heavy-chain-only antibodies derived from camelid serum. Compared with normal antibodies, nanobodies offer several advantages, including their small size, low immunogenicity, ability to recognize more cryptic antigenic sites within the CDR3 region, and stronger affinity, all of which make them widely used in disease treatment [8, 9]. Nanoantibodies targeting PD-L1 have emerged as a significant research area in tumor immunotherapy. Furthermore, the compact size of nanobodies simplifies the design and preparation of CARs, and their ability to identify cryptic antigen sites enhances the targeting effectiveness of CARs [10]. Accordingly, the integration of nanobody technology into tumor immunotherapy, particularly through the strategic targeting of PD-L1, represents a pivotal advance. Besides, the major histocompatibility complex class I-related chain A/B (MICA/B) genes serve as ligands for the activating receptor NKG2D on NK cells. However, during the progression of tumor growth and development, MICA/B is prone to proteolytic shedding from the cell surface, leading to its downregulation on tumor cell surfaces, facilitating immune escape [11]. NKG2D can respond to MICA/B on the tumor cell surface, potentially reducing the probability of immune escape and reversing the immunosuppressive effects [11].

Antigen loss, often caused by downregulation or mutation of target antigens shed on tumor cell surfaces, limits CAR function during tumor treatment using CAR technology [12]. To address this issue, researchers have developed dual-specificity CARs capable of recognizing two distinct target antigens, which may reduce the likelihood of immune evasion by tumor cells [13, 14]. Here, we rationally constructed a novel dual-targeted CAR (dtCAR), mainly containing PD-L1 nanobodies (PD-L1<sup>Nb</sup>) and an NKG2D activating receptor, which can target PD-L1 on the surface of cancer cells with high affinity and concurrently recognize MICA/B on the surface of tumor cells. This third-generation CAR structure incorporates the transmembrane segment of CD28 and costimulatory molecules 4-1BB and CD3 $\zeta$ , which are anticipated to transform inhibitory signals from PD-L1 and MICA/B into activating signals, thereby bypassing negative immune regulation. We examined whether NK92 cells expressing dtCAR can effectively and precisely target tumor cells, before investigating the underlying mechanisms by which dtCAR exerts its anti-tumor effects, both in vitro and in vivo.

## Methods

### Cell lines and cell culture

Cell lines were purchased from the American Type Culture Collection (ATCC, USA) and were maintained under

a humidified atmosphere of CO<sub>2</sub> at 37 °C. Human NK92 cells were incubated in alpha minimum essential medium (α-MEM, Hyclone, USA) containing L-Glutamine, ribonucleosides, deoxyribonucleosides, and 100 U/ml recombinant interleukin-2 (IL-2) (Peprotech, USA) and adjusted to a final concentration of 12.5% horse serum (Hyclone, USA), 12.5% fetal bovine serum (FBS; Biological Industries, Beit Haemek, Israel), 100 U/ml penicillin, and 100 µg/ml streptomycin (Beyotime Biotechnology, China). Cell lines were propagated as described in our previous work [15, 16].

#### DtCAR construction, lentivirus production, and transduction

We selected the full-length PD-L1 nanobody and a rationally designed extracellular domain of NKG2D (amino acids 82–216) to serve as antigen recognition domains, which are connected by a G<sub>4</sub>S linker (GGGSGGGSGGGGS) between them. NKG2D, through a monomeric mutant IgG4 hinge region (ESKY-GPPAPPAP), is connected to the transmembrane and intracellular segment of CD28 (amino acids 153–220), responsible for signal transmission. We selected the intracellular domain of 4-1BB (CD137, amino acids 214–255) and the intracellular segment of the CD3ζ chain (amino acids 52–164) as the intracellular signaling domains. To facilitate the exclusion of endogenous NKG2D interference from NK92 cells during flow cytometry sorting, a Flag tag (DYKDDDDK) was added to the N-terminus of PD-L1<sup>Nb</sup>. Ultimately, this construct assembled a dual-targeting CAR, designated as dtCAR, with the sequence configuration: Flag-PD-L1<sup>Nb</sup>-G<sub>4</sub>S Linker-NKG2D-CD28 TM-CD28 CP-4-1BB CP-CD3ζCP (from N-terminus to C-terminus). The constructs were subcloned into the lentivirus vector pCDH-CMV-MCS-P2A-copGFP-T2A-Puro.

NK92 cells were transduced using viral supernatant, with the resulting infected cell lines designated as NK92 and dtCAR-NK92. The transduction of NK92 cells was performed as described in our previous study [15].

#### Quantitative real-time PCR (qRT-PCR)

To detect the expression of dtCAR in CAR-NK92 and NK92 cells, total RNA was extracted and reverse-transcribed into cDNA. The mRNAs were detected using qRT-PCR as described in our previous study [19]. Glyceraldehyde-3-phosphate dehydrogenase (GAPDH) served as an internal control for normalization. The primer sequences used were as follows:

GAPDH sense: 5'-GAGGACCTGACCTGCCGTCT-3'.

GAPDH-antisense: 5'-GGAGGAGTGGGTGTCTGCTGT-3'.

PD-L1-sense: 5'- AGCGGCAAAATGAGCAGTAGA-3'.

PD-L1-antisense: 5'- AATCTGCCCTTCACAGAGTCG-3'.

NKG2D-sense: 5'- GGCTCCATTCTCTCACCCA-3'.

IgG4-antisense: 5'- GGTGCTGGAGGCCCACTATT-3'.

Linker sense: 5'-CCAGGGCACACAGGTGAC-3'.

Linker-antisense: 5'- AGGACATGGGCCACAGTAA-3'.

#### Flow cytometry analysis

To assess CAR surface expression and concurrently determine the presence of PD-L1 and MICA/MICB on the surfaces of H1299, SGC-7901, A549, and MGC-803 tumor cell lines, the following procedure was conducted: Cells were harvested, washed twice with 1x phosphate-buffered saline (PBS), and then stained with APC-conjugated mouse anti-NKG2D monoclonal antibodies (eBioscience, USA), APC-conjugated anti-PD-L1 monoclonal antibody (Invitrogen, USA), or PE-conjugated anti-human MICA/MICB antibody (eBioscience). Stained samples were analyzed using a Guava® easyCyte™ Flow Cytometer (Millipore, USA), and data were processed using FlowJo V10 software (FlowJo LLC, Ashland, USA).

#### Western blot analysis

For western blot analysis, cells were washed twice with 1×PBS, before adding protease inhibitors to the cell lysis buffer to preserve target proteins in the cell extract. Lysates were analyzed under denaturing conditions on 10% SDS-PAGE. The proteins on the SDS-PAGE gel were then transferred onto PVDF membranes. Membranes were blotted with transfer buffer for 45 min at room temperature and blocked with 5% skim milk for 1 h. The membranes were then incubated with an anti-FLAG antibody (Proteintech, 1:3000) for 1 h, before washing with TBST and incubating with HRP-conjugated anti-rabbit IgG secondary antibody (Proteintech, 1:3000) in 5% skim milk. After extensive washing, an imager was used for exposure.

#### Cell counting Kit-8

A CCK-8 assay was performed as previously described in our previous study [15].

#### In vitro cytotoxicity and release assays

A549, H1299, SGC-7901, and MGC-803 cells were cocultured with NK92 and dtCAR-NK92 cells at predetermined effector-to-target (E: T) ratios of 5:1 in triplicate wells in U-bottomed 96-well plates maintained at 37 °C. The cytotoxic capacity of NK cells was assessed using a luciferase assay, in which luciferase was utilized to infect cancer cells identically to the CAR introduction method.

Briefly, 10  $\mu$ L of lysis solution was added to the well representing the maximum lysis of target cells, while 10  $\mu$ g/mL of either NKG2D or PD-L1 antibody was introduced to the antibody-blocking group. After coincubation, the 96-well plate was retrieved, and 30  $\mu$ L of ONE-Glo™ Luciferase Assay reagent (Promega, USA) was administered to all test wells before luminometric measurement using a microplate reader. The formula for cytotoxicity was as follows: cytotoxicity (%) = (RLU\_min – RLU\_sample) / (RLU\_min – RLU\_max)  $\times$  100%.

In addition,  $1 \times 10^4$  target cells were incubated alongside  $5 \times 10^4$  effector cells in U-bottomed 96-well plates for a duration of 6–8 h. Thereafter, the culture supernatants were harvested and subjected to enzyme-linked immunosorbent assay (ELISA) for quantification of TNF- $\alpha$ , IFN- $\gamma$ , perforin, and Granzyme B release, adhering strictly to the guidelines provided by NEOBIOSCIENCE Co., Ltd., Shenzhen.

#### High-content cell imaging assay

Briefly, high-content cell imaging was conducted using the ImageXpress® Micro 4 High-Content Imaging System (Molecular Devices, Sunnyvale, CA), following the methodology outlined in our previous study [15].

#### Xenograft mouse model

Six- to eight-week-old female NCG mice (NOD/ShiLtJGpt-Prkdcem26Cd52Il2rgem26Cd22/Gpt; Gem Pharmatech, Nanjing, China) were maintained under specific pathogen-free (SPF) conditions with unlimited access to sterile water and food.

To establish the H1299 xenograft model,  $3.5 \times 10^6$  H1299 cells were resuspended in 100  $\mu$ L of PBS and inoculated subcutaneously into mice. Upon reaching a tumor volume of 65–100 mm<sup>3</sup> (calculated as volume = length  $\times$  width<sup>2</sup> / 2), the tumor-bearing mice were randomized and evenly distributed into three groups ( $n=6$  each): PBS, NK92 cells, and dtCAR-NK92 cells. Mice received injections via the tail vein with either  $1 \times 10^7$  NK92 cells or dtCAR-NK92 cells in 200  $\mu$ L of PBS or 200  $\mu$ L of PBS alone (administered every 7 days, for two doses). In addition, all mice received intraperitoneal injections of IL-2 (1000 U per mouse) thrice weekly. The tumor volumes and body temperatures were monitored concurrently throughout the study. Upon study termination, the mice were euthanized by cervical dislocation. And then the tumors, hearts, livers, lungs, spleens, kidneys, and other organs were harvested. Blood samples were collected for cytokine analysis by ELISA. This study strictly adhered to the Animal Management Rules of the Ministry of Health of the People's Republic of China and was approved by the Animal Ethics Committee of Xinxiang Medical University.

#### Statistical analysis

The unpaired two-tailed Student's t-test was used to compare the means of the two groups, as specified in each Fig. legend. All results were shown as the mean  $\pm$  standard deviation (SD). Following standard practice, statistical significance is defined as  $p < 0.05$ , whereas highly statistically significant differences are denoted by  $p < 0.001$ . All statistical analyses were performed using GraphPad Prism software (GraphPad, San Diego, CA, USA).

## Results

#### Rational design and construction of the dtCAR

Analysis of the crystal structure revealed that despite being a type II transmembrane protein, NKG2D retains its capacity to bind ligands when the extracellular domain's 82–216 amino acids are selected and paired with a type I transmembrane configuration. Incorporating the IgG4 hinge region ensures that NKG2D's entire extracellular portion approximates its native conformation, enhancing the stability of the molecular complex in the extracellular environment. PD-L1<sup>Nb</sup> exhibits minimal additional folding requirements and remains unaffected by the transmembrane type. By attaching it to the N-terminus of NKG2D via a G<sub>4</sub>S linker, the near-native conformation of NKG2D is preserved, whereas PD-L1<sup>Nb</sup> leverages its high antigen affinity for rapid target cell recognition.

Based on 3D structure modeling analyses of PD-L1<sup>Nb</sup> and the NKG2D extracellular domains, the AlphaFold2 tool was used to predict the structure of dtCAR (Fig. 1A). Structural analysis revealed a high similarity between PD-L1<sup>Nb</sup> (TM-score = 0.90) and NKG2D (TM-score > 0.95) in dtCAR compared with their respective original crystal structures, suggesting that dtCAR maintains conformations conducive to ligand binding.

As depicted in Fig. 1B, the dtCAR construct incorporates the full-length PD-L1<sup>Nb</sup>, situating distally from the membrane and linked to NKG2D's extracellular segment via a G<sub>4</sub>S linker, which is further associated with the transmembrane and intracellular segments of CD28, the intracellular region of 4-1BB (CD137), and the intracellular fragment of CD3 $\zeta$ . To prevent interference during cell sorting due to endogenous NKG2D, a FLAG tag (DYKDDDDK) was introduced at PD-L1<sup>Nb</sup>'s N-terminus. The dtCAR gene was engineered into an expression vector accompanied by GFP to facilitate the isolation of monoclonal cell lines in subsequent stages. In addition, the qRT-PCR and flow cytometry results verified the expression of dtCAR, PD-L1<sup>Nb</sup>, and NKG2D in NK92 cells (Fig. 1C–F), confirming the successful generation of dtCAR-engineered NK92 cells.

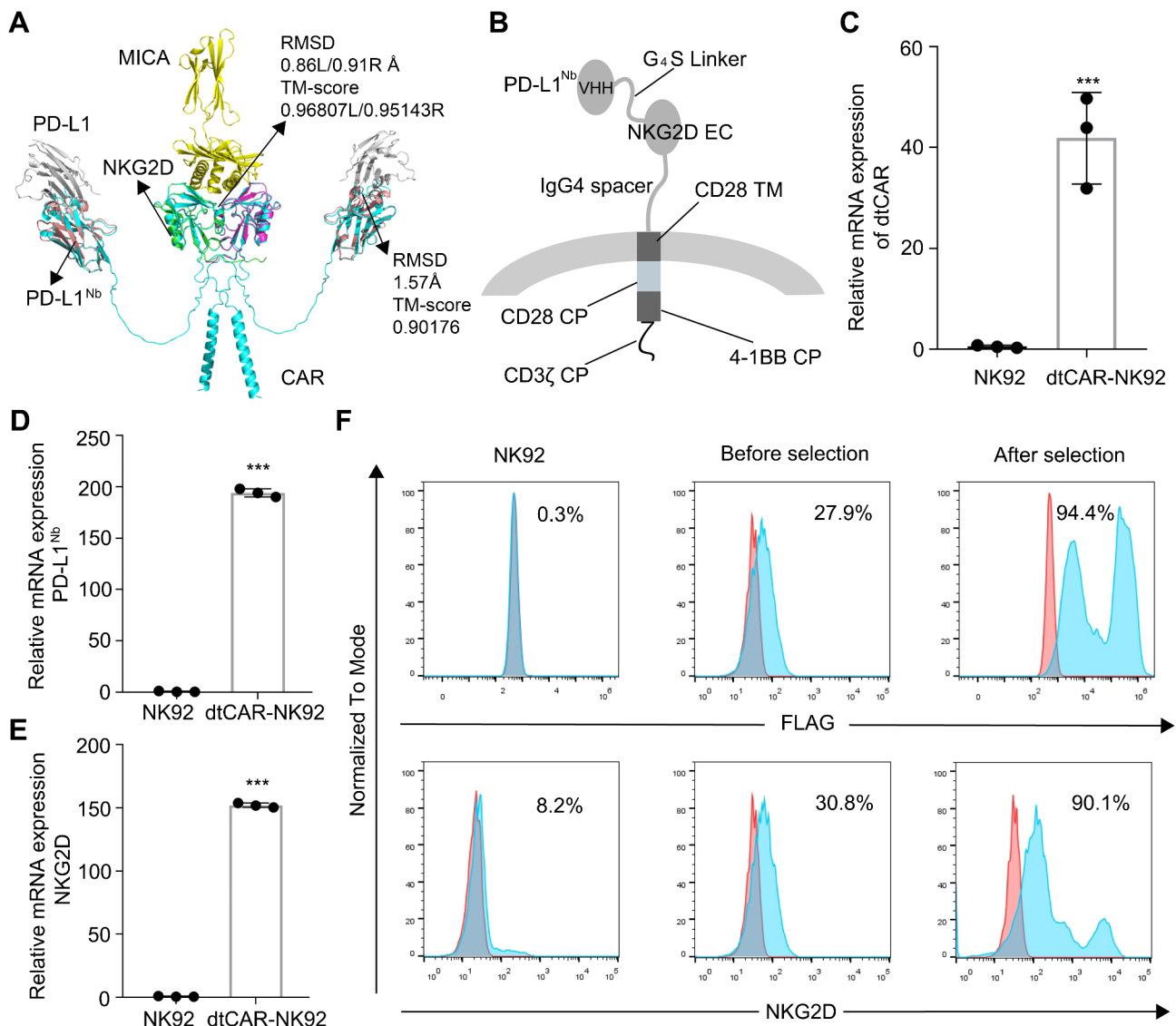


**Fig. 1** Rational construction and expression profiles of dtCAR. **(A)** The three-dimensional structures of dtCAR (cyan) and their interactions with PD-L1 (gray) and MICA (yellow) are shown. PD-L1<sup>Nb</sup> (PDB identifier 5JDS) is colored pale pink. NKG2D (PDB identifier 1HYR) is colored green and magenta. The protein structures were predicted using AlphaFold2, aligned using TM-align, and displayed using PyMOL v2.2.3 software. **(B)** Schematic diagram of dtCAR showing the extracellular (EC), transmembrane (TM), and cytoplasmic (CP) domains. **(C, D, E)** qRT-PCR analysis of dtCAR, PD-L1<sup>Nb</sup>, and NKG2D expression in NK92 and dtCAR-NK92 cells, respectively. **(F)** The expression of dtCAR in NK92 cells was analyzed via staining with anti-FLAG and NKG2D antibodies. Each experiment was performed with three independent replicates. Data are presented as the mean  $\pm$  SD. Statistical analysis was performed using a two-tailed Student's t-test; \*\*\* $p < 0.001$

### Characterization and specific cytotoxicity of dtCAR-engineered NK92 cells

To verify whether the modified dtCAR-NK92 cells maintain the molecular phenotype and proliferative capacity of parental NK92 cells, flow cytometry was used to detect the expression levels of the representative phenotypic molecules CD56, CD16, and CD3 in both dtCAR-NK92 and NK92 cells (Fig. 2A). The proliferation abilities of dtCAR-NK92 and NK92 cells were assessed using a CCK8 assay (Fig. 2B). The results showed that the

modified dtCAR-NK92 cells had similar phenotype and proliferation capacity with the parental NK92 cells.

To assess whether genetically modified NK92 cells display increased cytotoxicity, four tumor cell lines with different levels of PD-L1 and MICA/MICB expression were used. The PD-L1 expression in MGC-803, H1299, A549, and SGC-7901 cells was 2.6%, 67.3%, 24.4%, and 56.1%, whereas the MICA/MICB expression was 58%, 96.1%, 7.3%, and 61.2%, respectively (Fig. 2C). While NKG2D recognizes MICA/B, and other NKG2D ligands, we quantified the expression levels of other NKG2D ligands



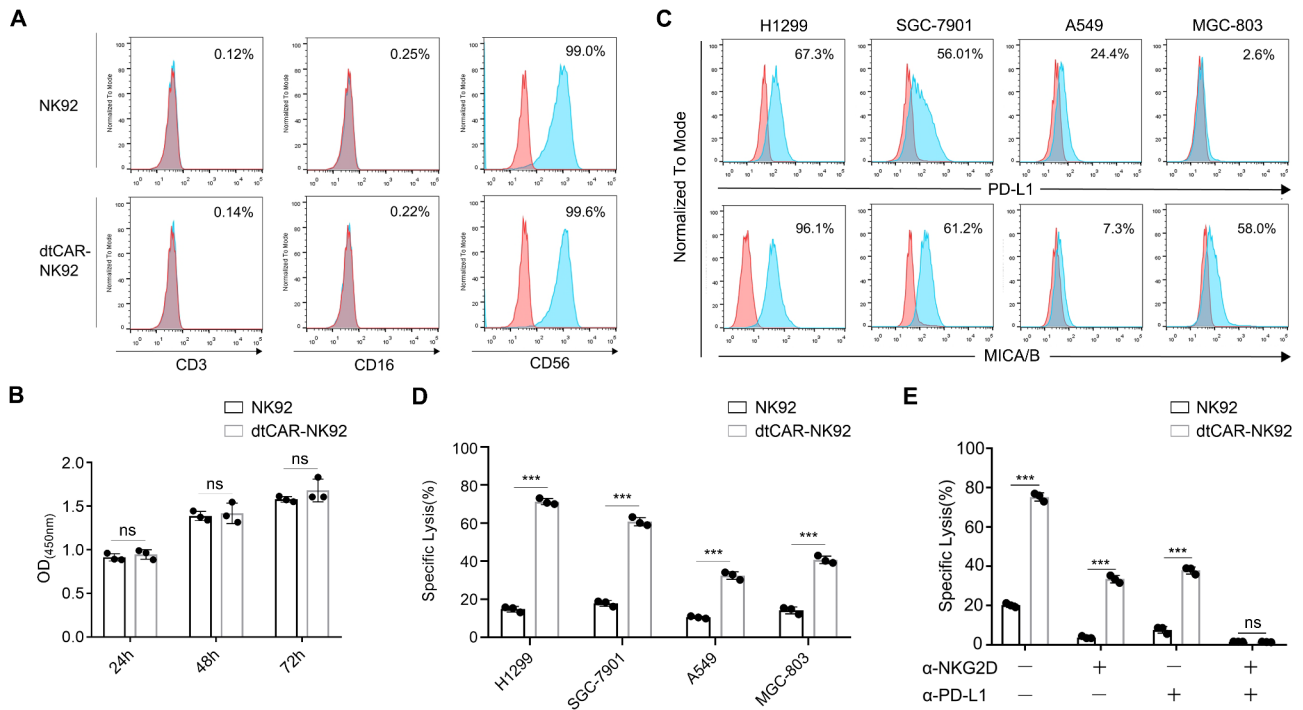


**Fig. 2** Phenotypic characterization and in vitro killing activity of dtCAR-NK92 cells. **(A)** The surface expression of phenotypic molecules on dtCAR-NK92 cells was analyzed by flow cytometry after staining with appropriate antibodies. **(B)** The proliferation of NK92 cells transduced with dtCAR was compared with parental NK92 cells using a CCK-8 assay. **(C)** Flow cytometry was used to analyze tumor cells stained with anti-PD-L1 and anti-MICA/MICB antibodies. **(D)** The cytotoxicity of dtCAR-NK92 cells was measured using the luciferase assay at effector-to-target ratios (E/T) of 5:1. **(E)** Assessment of the cytotoxicity of NKG2D- or PD-L1-blocked NK92 and dtCAR-NK92 cells against H1299 cells. Each experiment was performed with three independent replicates. Data are presented as the mean  $\pm$  SD. Statistical analysis was performed using a two-tailed Student's t-test; \*\* $p < 0.05$ , \*\*\* $p < 0.001$ , ns: No significance

on the tumor cells (Supplementary Fig. S1). The cytotoxicity of NK92 and dtCAR-NK92 cells against tumor cells was tested at an effector-to-target ratio (E: T) of 5:1 using a luciferase assay. The killing effects of dtCAR-NK92 on the four cell lines were higher than those of parental NK92 cells (Fig. 2D). dtCAR-NK92 cells achieved a 71.32% killing effect on H1299 cells but only 60.78%, 40.78%, and 32.45% on SGC-7901, MGC-803, and A549 cells, respectively. The data indicate that dtCAR-NK92 cells are more effective against tumor cells expressing high levels of PD-L1 and MICA/B.

To determine whether dtCAR-NK92 cells act as OR logic gates, PD-L1<sup>Nb</sup> and NKG2D were blocked with antibodies at an E: T ratio of 5:1. The cytotoxicity of NK92 and dtCAR-NK92 cells against PD-L1- and MICA/B-positive H1299 cells was then evaluated (Fig. 2E). Blocking with NKG2D or PD-L1 antibodies reduced the killing efficiency of NK92 cells to approximately 5% and 10% and that of dtCAR-NK92 cells from 75.31 to 33.41% and 37.84%, respectively. Besides, the dtCAR-NK92 cells exhibited a similar killing efficiency to that of NK92 cells when both NKG2D and PD-L1 were simultaneously blocked. In addition, we also measured the cytotoxic effects of NK92 cells engineered with single-targeting CAR (PD-L1 or MICA/B alone) and dtCAR against

H1299 cancer cells (Supplementary Fig. S2). The data clearly demonstrated the enhanced efficacy of the dual-targeting approach compared to single-targeting CARs. Collectively, these findings suggest that dtCAR-NK92 cells are capable of recognizing and killing H1299 cells through either NKG2D or PD-L1 alone, and their killing efficiency is enhanced when both targets are present, indicating a synergistic effect.

#### Tumor cell killing mechanism induced by dtCAR-NK92 cells

To further investigate the mechanism by which CAR-NK cells exert their cytotoxic effects on H1299 cancer cells, a high-content imaging system was utilized to document the dynamic killing process of both NK92 and dtCAR-NK92 cells as they interacted with H1299 cells.

When H1299 tumor cells were co-cultured with dtCAR-NK92 cells, it seems that the two phenomena of pyroptosis and apoptosis was observed (Fig. 3A–C and Supplementary Video S1, S2 and S3). Pyroptosis can be differentiated from apoptosis based on morphological changes in H1299 cells, such as initial swelling followed by shrinkage. Recent studies have shown that gasdermin D (GSDMD) and gasdermin E (GSDME) in tumor cells can induce pyroptosis in response to chemotherapy drugs or CAR T cells [20, 21]. We then confirmed

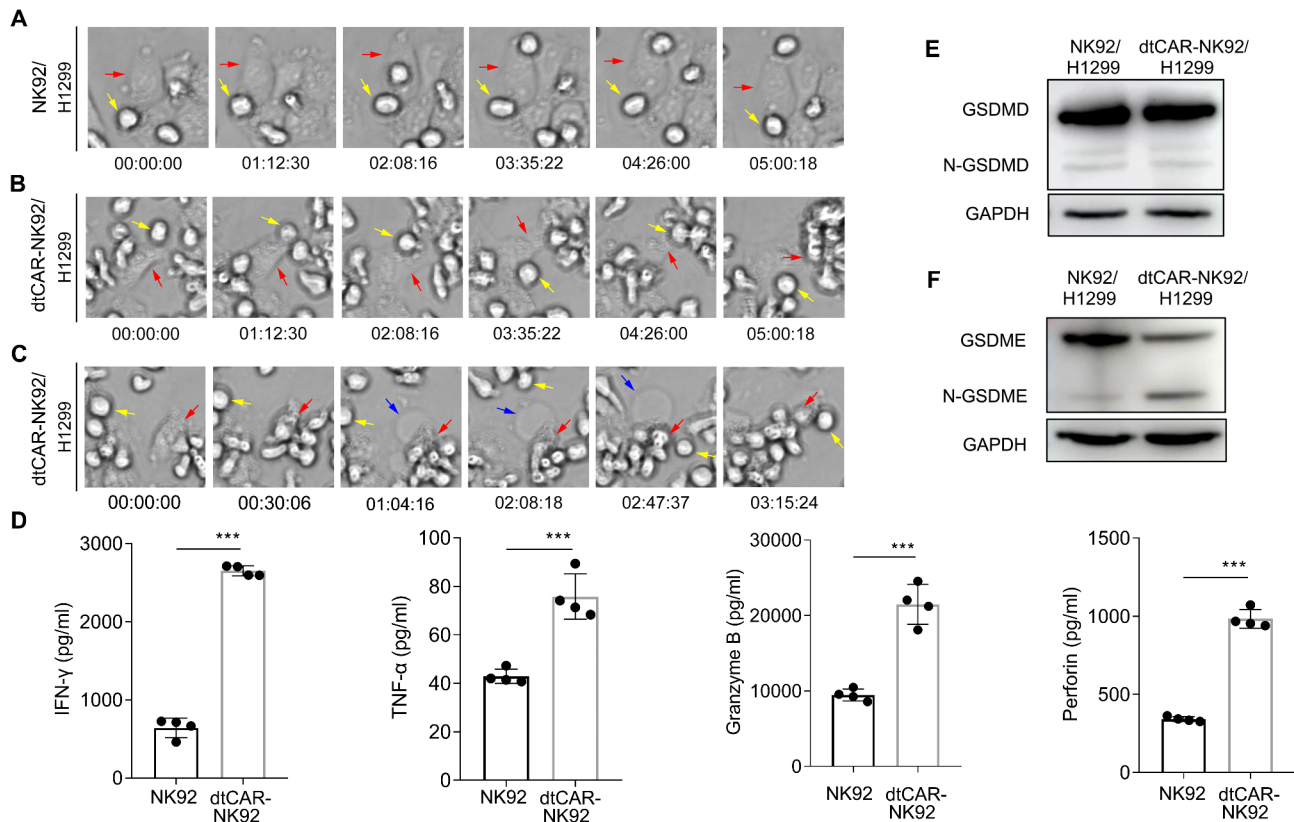


**Fig. 3** Mechanism of tumor cell clearance by dtCAR-NK92 Cells. (A–C) The kinetics of cytotoxicity of dtCAR-NK92 and NK92 cells against H1299 cells were captured using a high-content cell imaging system. Yellow arrows indicate NK92 cells and dtCAR-NK92 cells, while red arrows indicate H1299 cells. The blue arrows indicate pyroptotic H1299 cells. (D) Cytokine secretion was measured by ELISA. Each experiment was performed with three independent replicates. Data are presented as the mean  $\pm$  SD. (E–F) GSDMD, N-GSDMD, GSDME, and N-GSDME were determined by western blot when H1299 tumor cells were co-cultured with dtCAR-NK92 cells. Statistical analysis was performed using a two-tailed Student's t-test; \*\*\* $p < 0.001$

GSDME and GSDMD expression in H1299 cells. Western blotting analysis revealed that both GSDME and GSDMD were expressed in H1299 tumor cells; however, only N-GSDME was detected when H1299 cells were co-cultured with dtCAR-NK92 cells (Fig. 3E–F). Therefore, dtCAR-NK92 cells might induce GSDME-dependent pyroptotic death of H1299 cells.

We also investigated the secretion levels of major cytokines using an in vitro cytotoxicity assay to elucidate the mechanism by which dtCAR enhanced the killing activity of NK92 cells. The release of perforin, granzyme B, TNF- $\alpha$ , and IFN- $\gamma$  from H1299 cells was measured using an ELISA (Fig. 3D). The levels of cytokines released by dtCAR-NK92 cells post-killing H1299 cells were significantly higher than those released by NK92 cells. Taken together, our results suggest that pyroptosis is the primary mechanism responsible for the clearance of H1299 tumor cells by dtCAR-NK92 cells.

#### dtCAR-NK92 cells exhibit tumor regression and cytotoxicity in in vivo H1299 models

To assess the tumor regression capabilities of dtCAR-NK92 cells in vivo, a xenograft model was established

by subcutaneously injecting H1299 human lung cancer cells into NCG mice. dtCAR-NK92 and NK92 cells were injected twice weekly for 2 weeks (with dose escalation as appropriate) (Fig. 4A). Five days after the injection of tumor cells, mice with tumors were treated, and we regularly measured the dimensions of the tumors using calipers to monitor their growth. For NCG mice engrafted with human H1299 cells and subsequently treated with dtCAR-NK92 cells, a significant decrease in both tumor volume and tumor weight was observed compared with mice treated with non-transduced NK92 cells or PBS (Fig. 4B–D). In comparison, no significant difference in tumor size was observed between NCG mice engrafted with human H1299 cells treated with PBS and those treated with non-transduced NK92 cells. The results indicated that dtCAR-NK92 cells had inhibitory effects on tumor growth in mice, as depicted in Fig. 4C.

In addition, we further confirmed whether dtCAR-mediated in vivo killing was accompanied by high levels of cytokine secretion in mouse serum. Data showed that the dtCAR-NK92 cell treatment group exhibited higher secretion levels of cytokines than the PBS treatment group. The dtCAR group had higher granzyme B and

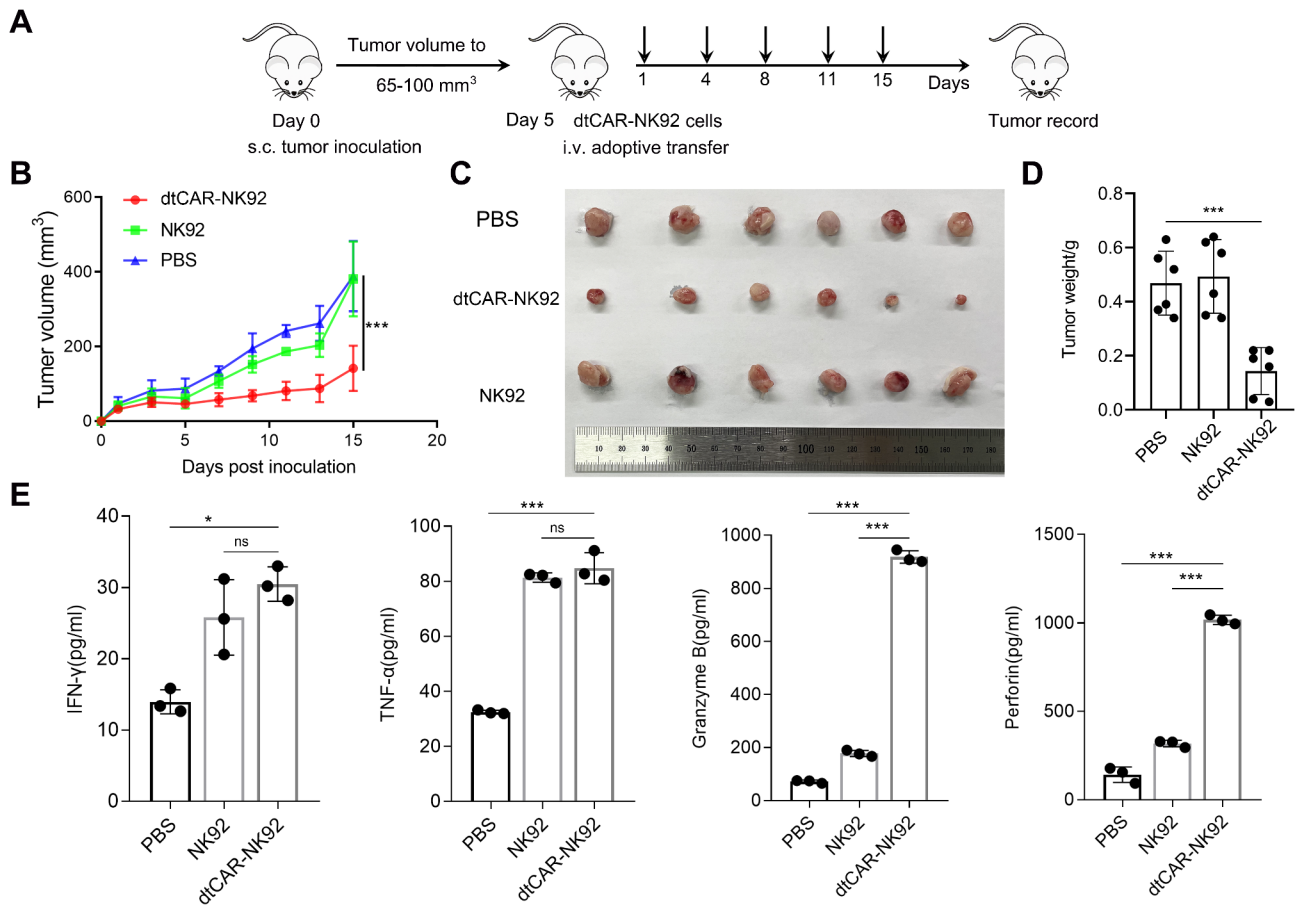


**Fig. 4** Superior activity of dtCAR-NK92 cells against lung cancer in vivo. **(A)** Schematic of in vivo studies in the H1299-bearing mouse xenograft model treated with PBS, NK92 cells, or dtCAR-NK92 cells. **(B)** The tumor growth curves of each treatment group were monitored throughout the study. Data are presented as the mean  $\pm$  SD. Statistical analysis was conducted using one-way analysis of variance followed by the Bonferroni test. \*\*\* $P < 0.001$ . **(C)** Resected tumors from each group were imaged at the end of the experiment. **(D)** The tumor weights for each group were measured and calculated upon the conclusion of the study. **(E)** The cytokine secretion levels for each group were determined. Statistical analysis was conducted using Student's t-test. \* $p < 0.05$ , \*\*\* $p < 0.001$ ; ns: No significance

perforin secretion levels than the NK92 group (Fig. 4E). These findings confirmed that dtCAR-NK92 cells exhibited great potential for suppressing the growth of H1299 cells in subcutaneous models.

## Discussion

Cellular, or adoptive immunotherapy, constitutes the fourth pillar of cancer immunotherapy following surgery, radiation, and chemotherapy by harnessing the immune system's capacity to eradicate tumors. CAR T-cell therapy has made substantial advancements in certain cancer treatments, but it faces challenges, primarily therapy failure, due to target antigen downregulation or loss. By contrast, CAR-NK cells retain inherent antitumor capabilities and can operate independently of the CAR, thereby potentially overcoming issues such as target antigen modulation, enhancing therapeutic outcomes, and minimizing treatment failures [17–20].

In this study, we rationally designed a dual-targeted CAR strategy inspired by the success of dual-targeted CD19 and CD20 CAR-T cells in B lymphocytic malignancies [21]. The novel dtCAR, which mainly contains PD-L1<sup>Nb</sup> and the NKG2D activating receptor, can target PD-L1 on the surface of cancer cells with high affinity and concurrently recognize MICA/B on the surface of tumor cells. The integration of camelid nanoantibodies into CAR designs represents a significant innovation, with preclinical studies validating nanoantibody-CAR-NK applications [22–24]. This dual-targeting strategy effectively overcomes the limitations of single-target CARs, which may fail to induce robust activation or lead to immune escape due to antigen loss. Meanwhile, this strategy is particularly important in solid tumors, where single-target CARs often face challenges due to tumor heterogeneity and immune evasion mechanisms. Specifically, the expression of multiple NKG2D ligands (MICA/B, ULBP1-6) on tumor cells suggests that our



dual-targeting CAR design could be activated through multiple pathways. This redundancy enhances the robustness of CAR activation and reduces the likelihood of immune escape through ligand downregulation. This mechanistic insight underscores the multifaceted nature of NKG2D-mediated immune activation and further supports the rationale for targeting MICA/B in our dual-targeting strategy.

Rapid dtCAR-NK92 cell clustering around cancer cells confirmed the PD-L1<sup>Nb</sup> design intent, but the correlation and mechanism require further exploration. Although NKG2D receptors on NK cells facilitate cytotoxicity and cytokine production, their activation alone may be insufficient for IFN- $\gamma$  production [25]. The incorporation of NKG2D into CAR structures to enhance NK cell therapy for solid tumors aligns with experimental evidence demonstrating enhanced functionality in modified NK cells [26].

Understanding the spatial conformation of ligand–receptor interactions prompts reconsideration of the extracellular domain length in CAR structures and its potential impact on killing efficiency [27]. This insight guides CAR structural optimization and extracellular segment design. Lentiviral vectors, which are used for NK92 cell transfection, exhibit low genotoxicity and stable integration, yet their low transfection efficiency may necessitate strategy adjustments for consistent expression verification [28, 29]. Our data illustrated that dtCAR modification did not alter NK92 cell proliferation or surface marker expression, confirming the safety and feasibility of dtCAR in enhancing the anti-tumor properties of NK92.

In vitro, cytotoxicity assays demonstrated that dtCAR-NK92 cells surpassed parental NK92 cells in eliminating various cancer lines, particularly H1299 cells with high PD-L1 and MICA/B expression, and even showed improvement in A549 cells with low expression levels. Effectiveness was also observed in single-positive PD-L1 or MICA/B cells, indicating versatile functionality. Blocking experiments revealed that both targets are crucial for the synergistic activation and optimal killing of dtCAR-NK92, suggesting a dual-target recognition mechanism. Next, we will clarify the underlying mechanisms by which dual targeting may confer advantages. This could involve exploring how targeting both PD-L1 and MICA/B might overcome immune evasion strategies employed by cancer cells, lead to more robust NK-cell activation, or reduce off-target effects compared to single-targeting CARs.

The evolution of the CAR design, incorporating costimulatory domains such as CD28 and 4-1BB, has improved cell persistence and cytotoxicity [21, 22]. While our data suggested that the CD28/4-1BB combination provides a robust activation profile for our NK cell-based CAR system, NK cell-specific costimulatory domains

(e.g., 2B4 or DAP10) remain potential candidates for specific CAR designs. Besides, we remain open to further optimization and are currently exploring the potential benefits of incorporating additional NK cell-specific costimulatory domains into our CAR design to further enhance its therapeutic potential. dtCAR-NK92 cells not only increased cancer cell killing but also secreted higher levels of cytokines such as IFN- $\gamma$ , TNF- $\alpha$ , perforin, and granzyme B. High-content imaging revealed that dtCAR-NK92 cells induced both apoptosis and pyroptosis in cancer cells, accompanied by cytokine secretion. Studies have suggested that certain cytokines, such as TNF- $\alpha$  or granzyme B, can activate caspase-3, which in turn promotes GSDME protein cleavage, thereby triggering cell pyroptosis [30, 31]. Our data suggest that dtCAR-NK92 cells induce GSDME-dependent pyroptotic death of H1299 cells. To further analyze the mechanism underlying dtCAR-NK92 cell killing, we plan to clarify which inflammatory caspase activates GSDM family members and cleaves them to produce its active form, thus triggering dtCAR-NK92 cell-induced pyroptosis.

In vivo, dtCAR-NK92 cells significantly controlled H1299 tumor growth with increased cytokine secretion. Enhanced NKG2D expression likely contributes to perforin and granzyme B secretion, influenced by its role in the MAPK pathway [32]. The variability in cytokine secretion between in vitro and in vivo may be related to CAR structure, tumor heterogeneity, and the complex TME, highlighting areas for further investigation. In addition, we will further validate these results in in vivo animal models, which will clearly demonstrate the superiority of our dual-targeting design over single-targeting CARs in terms of anti-tumor efficacy. Furthermore, demonstrating the survival benefit of dtCAR in the H1299 cancer cell line mouse model may also be important. but unfortunately, due to the limitations of our current study design and the complex nature of the H1299 model, we focused on several aspects of dtCAR NK cell function and did not directly assess the survival benefit in this specific model. While the current data provide valuable insights into the therapeutic potential of dtCAR-NK cells, regarding the assessment of dtCAR-NK cell engraftment and persistence and the evaluation of tumor infiltration, regrettably, due to limitations in the scope of our initial study and the resources available at the time, we did not include this specific analysis in the current study. However, we fully acknowledge their importance and plan to incorporate them into our future experiments. Besides, expanding the scope of our research to include additional cell lines and, if possible, primary tumours, would significantly strengthen our findings. Notably, adoptive immunotherapy against solid tumors involves multi-level strategies beyond cell-killing enhancement, including TME manipulation to promote immune cell infiltration

[33]. Future immunotherapies may focus on reprogramming the TME safely, highlighting the need for comprehensive approaches to effectively combat solid tumors.

## Conclusions

Here, we demonstrate that the expression of a novel dtCAR in NK92 cells mediates significant in vitro cytotoxicity and in vivo tumor control in H1299 human lung cancer cells. The rapid clearance of H1299 cells might be attributed to extensive pyroptosis induced by dtCAR-NK92 cells. Furthermore, this approach offers meaningful theoretical advantages for introducing NK-tailored chimeric receptors and suggests a potential route for the clinical treatment of lung cancer.

## Abbreviations

CAR	Chimeric antigen receptor
CP	Cytoplasmic
CRS	Cytokine release syndrome
dtCAR	Dual-targeted CAR
E:T	Effector-to-target
EC	Extracellular
GvHD	Graft-versus-host disease
MHC	Major histocompatibility complex
NK	Natural killer
PD-1	Programmed death receptor 1
PD-L1 <sup>Nb</sup>	PD-L1 nanoantibodies
qRT-PCR	Quantitative real-time PCR
TM	Transmembrane
TME	Tumor microenvironment

## Supplementary Information

The online version contains supplementary material available at <https://doi.org/10.1186/s12885-025-13780-2>.

Supplementary Material 1  
Supplementary Material 2  
Supplementary Material 3  
Supplementary Material 4  
Supplementary Material 5

## Acknowledgements

We wish to thank the Stem Cell and Biotherapy Engineering Research Center of Henan, affiliated with Xinxiang Medical University, for providing the lentiviral vector system. We thank LetPub ([www.letpub.com.cn](http://www.letpub.com.cn)) for its linguistic assistance during the preparation of this manuscript.

## Author contributions

L.Z. conceptualized the study, designed experiments, prepared figures, wrote the manuscript, and secured funding for the study. Z.Z. and Q.G. conceived and conducted the experiments and analyzed the data. C.S. and W.H. performed the Western blot assays and data analysis. Y.W. reviewed and edited the manuscript. C.G. and Z.N. contributed to the experimental design and reviewed the manuscript. W.Z. conceptualized and supervised the project. All authors reviewed the manuscript.

## Funding

This research was funded by the Henan Provincial Science and Technology Research and Development Joint Fund (Industrial) (grant number 235101610047, to W.Z.) the Henan Program for Science and Technology Development (grant number 232102311042 to L.Z.), and the Talent Support Program of Xinxiang Medical University (grant number XYBSKYZZ201924 to L.Z.).

## Data availability

Data is provided within the manuscript or supplementary information files.

## Declarations

### Ethics approval and consent to participate

The animal study protocol was approved by the Animal Ethics Committee of Xinxiang Medical University.

### Consent for publication

Not applicable.

### Competing interests

The authors declare no competing interests.

Received: 7 November 2024 / Accepted: 20 February 2025

Published online: 25 February 2025

## References

1. Siegel RL, Miller KD, Wagle NS, Jemal A. Cancer statistics, 2023. *CA Cancer J Clin.* 2023;73(1):17–48. <https://doi.org/10.3322/caac.21763>
2. Hanahan D. Hallmarks of cancer: new dimensions. *Cancer Discov.* 2022;12(1):31–46. <https://doi.org/10.1158/2159-8290.CD-21-1059>
3. Figueroa JA, Reidy A, Mirandola L, et al. Chimeric antigen receptor engineering: a right step in the evolution of adoptive cellular immunotherapy. *Int Rev Immunol.* 2015;34(2):154–87. <https://doi.org/10.3109/08830185.2015.1018419>
4. Sterner RC, Sterner RM. CAR-T cell therapy: current limitations and potential strategies. *Blood Cancer J.* 2021;11(4):69. <https://doi.org/10.1038/s41408-021-00459-7>
5. Fabian KP, Padgett MR, Donahue RN, et al. PD-L1 targeting high-affinity NK (t-haNK) cells induce direct antitumor effects and target suppressive MDSC populations. *J Immunother Cancer.* 2020;8(1):e000450. <https://doi.org/10.1016/j.jitc.2019.11.033>
6. Fabian KP, Padgett MR, Donahue RN, et al. PD-L1 targeting high-affinity NK (t-haNK) cells induce direct antitumor effects and target suppressive MDSC populations. *J Immunother Cancer.* 2020;8(1):e000450. <https://doi.org/10.1136/jitc-2019-000450>
7. Park JE, Kim SE, Keam B, et al. Anti-tumor effects of NK cells and anti-PD-L1 antibody with antibody-dependent cellular cytotoxicity in PD-L1-positive cancer cell lines. *J Immunother Cancer.* 2020;8(2):e000873. <https://doi.org/10.1136/jitc-2020-000873>
8. Hamers-Casterman C, Atarhouch T, Muyldermans S, et al. Naturally occurring antibodies devoid of light chains. *Nature.* 1993;363(6428):446–8. <https://doi.org/10.1038/363446a0>
9. Xie YJ, Dougan M, Jaikhan N, et al. Nanobody-based CAR T cells that target the tumor microenvironment inhibit the growth of solid tumors in immunocompetent mice. *Proc Natl Acad Sci U S A.* 2019;116(16):7624–31. <https://doi.org/10.1073/pnas.1817147116>
10. Mo F, Duan S, Jiang X, et al. Nanobody-based chimeric antigen receptor T cells designed by CRISPR/Cas9 technology for solid tumor immunotherapy. *Signal Transduct Target Ther.* 2021;6(1):80. <https://doi.org/10.1038/s41392-021-00462-1>
11. Zhang J, Basher F, Wu JD. NKG2D ligands in tumor immunity: two sides of a coin. *Front Immunol.* 2015;6:97. <https://doi.org/10.3389/fimmu.2015.00097>
12. Spiegel JY, Patel S, Muffly L, et al. CAR T cells with dual targeting of CD19 and CD22 in adult patients with recurrent or refractory B cell malignancies: a phase 1 trial. *Nat Med.* 2021;27(8):1419–31. <https://doi.org/10.1038/s41591-021-01436-0>
13. Thieblemont C, Phillips T, Ghesquieres H, et al. Epcoritamab, a novel, subcutaneous CD3xCD20 bispecific T-cell-engaging antibody, in relapsed or refractory large B-cell lymphoma: dose expansion in a phase I/II trial. *J Clin Oncol.* 2023;41(12):2238–47. <https://doi.org/10.1200/JCO.22.01725>
14. Grada Z, Hegde M, Byrd T, et al. TanCAR: a novel bispecific chimeric antigen receptor for cancer immunotherapy. *Mol Ther Nucleic Acids.* 2013;2(7):e105. <https://doi.org/10.1038/mtna.2013.32>
15. Guo C, Wang X, Zhang H, et al. Structure-based rational design of a novel chimeric PD1-NKG2D receptor for natural killer cells. *Mol Immunol.* 2019;114:108–13. <https://doi.org/10.1016/j.molimm.2019.07.009>

16. Guo C, Guo X, Li X, et al. The SpyCatcher-SpyTag interaction mediates tunable anti-tumor cytotoxicity of NK cells. *Mol Immunol*. 2024;165:11–8. <https://doi.org/10.1016/j.molimm.2023.12.001>
17. Zhi L, Wang X, Gao Q, et al. Intrinsic and extrinsic factors determining natural killer cell fate: phenotype and function. *Biomed Pharmacother*. 2023;165:115136. <https://doi.org/10.1016/j.biopha.2023.115136>
18. Oei VYS, Siernicka M, Graczyk-Jarzynka A, et al. Intrinsic functional potential of NK-cell subsets constrains retargeting driven by chimeric antigen receptors. *Cancer Immunol Res*. 2018;6(4):467–80. <https://doi.org/10.1158/2326-6066.CIR-17-0207>
19. Sun C, Sun H, Zhang C, Tian Z. NK cell receptor imbalance and NK cell dysfunction in HBV infection and hepatocellular carcinoma. *Cell Mol Immunol*. 2015;12(3):292–302. <https://doi.org/10.1038/cmi.2014.91>
20. Sung PS, Jang JW. Natural killer cell dysfunction in hepatocellular carcinoma: pathogenesis and clinical implications. *Int J Mol Sci*. 2018;19(11):3648. <https://doi.org/10.3390/ijms19113648>
21. Zah E, Lin MY, Silva-Benedict A, Jensen MC, Chen YY. T cells expressing CD19/CD20 bispecific chimeric antigen receptors prevent antigen escape by malignant B cells. *Cancer Immunol Res*. 2016;4(6):498–508. <https://doi.org/10.1158/2326-6066.CIR-15-0231>
22. Xie G, Dong H, Liang Y, Ham JD, Rizwan R, Chen J. CAR-NK cells: a promising cellular immunotherapy for cancer. *EBioMedicine*. 2020;59:102975. <https://doi.org/10.1016/j.ebiom.2020.102975>
23. Hambach J, Riecken K, Cichutek S, et al. Targeting CD38-expressing multiple myeloma and Burkitt lymphoma cells in vitro with nanobody-based chimeric antigen receptors (Nb-CARs). *Cells*. 2020;9(2):321. <https://doi.org/10.3390/cells9020321>
24. You F, Wang Y, Jiang L, et al. A novel CD7 chimeric antigen receptor-modified NK-92MI cell line targeting T-cell acute lymphoblastic leukemia. *Am J Cancer Res*. 2019;9(1):64–78.
25. Watzl C, Long EO. Signal transduction during activation and inhibition of natural killer cells. *Curr Protoc Immunol*. 2010;Chap 11:10.1002/0471142735.im1109bs90. <https://doi.org/10.1002/0471142735.im1109bs90>
26. Chang YH, Connolly J, Shimasaki N, Mimura K, Kono K, Campana D. A chimeric receptor with NKG2D specificity enhances natural killer cell activation and killing of tumor cells. *Cancer Res*. 2013;73(6):1777–86. <https://doi.org/10.1158/0008-5472.CAN-12-3558>
27. Xiao Q, Zhang X, Tu L, Cao J, Hinrichs CS, Su X. Size-dependent activation of CAR-T cells. *Sci Immunol*. 2022;7(74):eabl3995. <https://doi.org/10.1126/sciimmunol.abl3995>
28. Papayannakos C, Daniel R. Understanding lentiviral vector chromatin targeting: working to reduce insertional mutagenic potential for gene therapy. *Gene Ther*. 2013;20(6):581–8. <https://doi.org/10.1038/gt.2012.88>
29. Bari R, Granzin M, Tsang KS et al. A distinct subset of highly proliferative and lentiviral vector (LV)-transducible NK cells define a readily engineered subset for adoptive cellular therapy [published correction appears in *Front Immunol*. 2019;10:2784]. *Front Immunol*. 2019;10:2001. <https://doi.org/10.3389/fimmu.2019.02001>
30. Yao F, Jin Z, Zheng Z, et al. HDAC11 promotes both NLRP3/caspase-1/GSDMD and caspase-3/GSDME pathways causing pyroptosis via ERG in vascular endothelial cells. *Cell Death Discov*. 2022;8(1):112. <https://doi.org/10.1038/s41420-022-00906-9>. Published 2022 Mar 12.
31. Zhang Y, Cai X, Wang B, Zhang B, Xu Y. Exploring the molecular mechanisms of the involvement of GZMB-Caspase-3-GSDME pathway in the progression of rheumatoid arthritis. *Mol Immunol*. 2023;161:82–90. <https://doi.org/10.1016/j.molimm.2023.07.013>
32. Lu CC, Chen JK. Resveratrol enhances perforin expression and NK cell cytotoxicity through NKG2D-dependent pathways. *J Cell Physiol*. 2010;223(2):343–51. <https://doi.org/10.1002/jcp.22043>
33. van Ravenswaay Claassen HH, Kluin PM, Fleuren GJ. Tumor infiltrating cells in human cancer. On the possible role of CD16 + macrophages in antitumor cytotoxicity. *Lab Invest*. 1992;67(2):166–74.

## Publisher's note

Springer Nature remains neutral with regard to jurisdictional claims in published maps and institutional affiliations.